LA-UR- 01-4463

Approved for public release; distribution is unlimited.

Title: Supercritical Density Measurements of Laser Irradiated Ar Clusters

Author(s): Gwyneth C. Junkel-Vives, Joseph Abdallah, Jr., F. Blasco, F. Dorcies, T. Caillaud, C. Bonte, C. Stenz, F. Salin, A. Ya. Faenov, A.I. Magunov, T.A. Pikuz, I. Yu. Skobelev

Submitted to: Physical Review Letters

Los Alamos
NATIONAL LABORATORY

Preprint No.

Supercritical Density Measurements of Laser Irradiated Ar Clusters

G. C. Junkel-Vives[a], J. Abdallah, Jr.[a],F. Blasco[b],

F. Dorcies[b], T. Caillaud[b], C. Bonte[b],

C. Stenz[b], F. Salin[b], A. Ya. Faenov[c],

A. I. Magunov[c],T. A. Pikuz[c], I. Yu. Skobelev[c]

[a] *Theoretical Division, T-4, Los Alamos National Laboratory,*

P.O. Box 1663, Los Alamos NM 87545

[b] *CELIA, Université Bordeaux 1-CNRS, 33405 Talence, France*

[c] *Multicharged Ions Spectra Data Center of VNIIFTRI,*

Mendeleevo, 141570 Moscow region, Russia

(July 30, 2001)

Abstract

Plasmas have been created with supercritical electron densities ($N_e = 2 \times 10^{22}$ cm^{-3}) by irradiating atomic clusters of argon with a high contrast, ultrashort (<100 fs) laser pulse. This is the first time such densities have been measured for plasmas created from gas clusters. High resolution Ar K-shell spectra were obtained and analyzed using a theoretical two-temperature collisional-radiative model of irradiated atomic clusters incorporating the effects of highly energetic electrons (~5 keV). Results from trials using pulses on the order of 300-400 fs are also consistent with a hydrodynamic model of laser-cluster interaction.

Typeset using REVTEX

The interaction of high-power, ultra-short laser pulses with atomic gas clusters has been a subject of active investigation for a number of years and continues to be studied for a variety of applications and to gain insight into the behavior of matter under extreme conditions [1–11]. For example, laser irradiated clusters are relatively inexpensive, compact sources of extreme ultraviolet radiation (EUV) and x-rays. In addition, plasma conditions comparable to those obtained in large scale experiments, such as inertial confinement fusion and z-pinch, can be achieved by using relatively small experimental set-ups. Cluster-plasmas with electron densities higher than critical density have been inferred from bright x-ray emission due to rapid collisional heating. In fact, high plasma temperatures and densities distinguish laser interactions with clusters from interactions with gas targets [1]. The highest densities measured so far have been close to critical density for Ti:Sapphire lasers ($N_e = 1.7 \times 10^{21}$ cm^{-3}). Such densities were measured using detailed spectroscopic analysis [12–14].

Achieving higher, supercritical densities from laser irradiated clusters are of great interest for a variety of reasons. Achieving cluster-plasmas with supercritical densities would offer hope that laser irradiated clusters can be used as ultrafast (fs-ps) x-ray sources for time resolved x-ray diffraction experiments. In addition, such conditions would approximate isochoric plasmas, which are important for opacity experiments. A high density, moderate temperature (kT=100-200 eV) would also provide another example of a strongly coupled plasma [15].

In this paper we describe ultrashort laser experiments conducted on Ar clusters at the Celia laser installation at the University of Bordeaux, France, where electron densities of more than 10^{22} cm^{-3} were measured for the first time during a laser-cluster experiment, an order of magnitude greater than critical density, N_{crit}. Both contrast and pulse length were varied to determine their effects on plasma temperature, electron density and hot electron fraction. High resolution Ar K-shell emission spectra was obtained and analyzed using a collisional-radiative kinetics model incorporating the effects of hot electrons. Results from trials using pulses on the order of 300-400 fs are also consistent with the hydrodynamic model of laser-cluster interaction of Milchberg et al [16], which eliminates the uniform density

assumption of Ditmire's "nanoplasma" model.

The densities described aboved were obtained by using both high contrast and ultrashort (<100 fs) laser pulses. Laser prepulse and pulse length are two parameters shown to effect the development of laser-produced plasmas. The effect of prepulse on laser produced plasmas has been studied more in the context of solid targets, where a relatively low-contrast prepulse can help to create a high temperature plasma and consequently a bright source of x-rays [17–23]. In addition, a high contrast pulse allows the main pulse to interact with a solid density target, which is less efficient for absorbing laser energy, but is effective for creating ultrashort x-ray pulses [24–27]. Any laser system has a prepulse; however, it is well known that without specific modifications Ti:Sapphire laser systems like the one used in the current experiment have especially poor contrast. In the case of gas-jet clusters, a sufficiently strong prepulse could destroy a cluster, i. e. cause the cluster to expand to the density of the surrounding underdense plasma. As with a solid target, if a sufficiently high contrast pulse is used, the main pulse should be able to interact with the solid density clusters. A similar effect on the cluster is observed as pulse length is varied. It has been shown that there is optimum absorption of the laser energy if the cluster is given time to expand to critical density and maximize resonant heating, but not so much time that the density scale length increases to the point that it inhibits laser energy absorption at the critical density surface. [28,29,16]. On the other hand, an ultrashort pulse length allows the laser energy to be deposited before the cluster has a chance to expand, albeit less efficiently. As a result, a plasma characterized by a supercritical density can be formed.

The experiments presented here were carried out on the CELIA laser facility (Bordeaux, France). The experimental set-up is shown in Fig. 1. The laser source works at 1 Khz repetition rate and produces Terawatt level femtosecond pulses. A Ti:sapphire oscillator produces 11 fs pulses which are amplified in a series of four amplifiers. All four Ti:sapphire amplifiers are pumped by five Nd:YLF lasers running at 1 kHz. The pulse energy is about 15 mJ around 800 nm, and the pulse duration can be adjusted from 30 fs to several picoseconds. The laser pulse duration was changed by moving one of the two gratings of the compressor.

This chirped pulse compressor is based on the Treacy [30] theory. Pulse duration was controlled by a auto-correlator measurement system.

Pre-pulse formation in the regenerative amplifier four and nine nanoseconds before the main pulse has been prevented by using a Pockels cell. In the past [14,31], the Pockels cell was placed before the regenerative amplifier, and was used as a pulse picker. This configuration was not the best to prevent nanosecond pre-pulse: the nanosecond contrast ratio achieved was about 10^2-10^3. We now use a new configuration; we have placed the Pockels cell after the regenerative amplifier as a pulse cleaner. A contrast ratio better than 10^5 is obtained. The measured ASE background intensity is at least 8 orders of magnitude less than the laser pulse intensity. The pulse-to-pulse stability of our laser source was typically 2% rms. To avoid beam and compressor damage, the laser beam propagates in vacuum. A 5 μm laser spot radius is obtained in vacuum by using a 100 mm focal length, f/3 off-axis parabolic mirror. The maximum laser intensity on the target is 1.5×10^{17} W/cm^2.

Targets are produced in the vacuum chamber by a pulsed supersonic gas jet using a conical nozzle. Argon is a good choice for a target because K-shell emission is readily obtained and is more suitable for detailed spectroscopic analysis than krypton or xenon, which would yield more complex L- and M-shell spectra. The radial density profile and cluster size were measured (see for more details [32]) by means of Rayleigh scattering and using Mach-Zender interferometry and also calculated using mathematical model of two-phase gas flow [33]. The laser pulse was focused onto the gas jet target at a distance of 1.5 mm from the nozzle output. The maximum backing pressure was 63 bar for the current experiment. For such experimental conditions measured and calculated Ar cluster size is reached up to 0.03-0.04μm and the average number of Ar atoms per cluster reaches about 5×10^6

The x-ray spectral measurements were conducted using so called Focusing Spectrometers with Spatial Resolution (FSSR) spectrometers and is described in detail in Ref. [34]. In our case for such spectrometer a spherically bent mica crystal (R=100 mm) was ued to image the x-rays onto a X-ray CCD camera [31]. The spectrometer was placed in two different

orientations, which allowed us to receive spectral images of the plasma with spatial resolution in the direction of laser propagation or in perpendicular direction (see Fig. 1). For the current investigations, the spectral region of 3-4.2 Å was studied. The x-ray spectrum in the region of the Ar $Ly_\alpha He_\alpha$ was recorded using 2000 laser shots. The spectral resolution of the spectrographs was about $\lambda/\Delta\lambda = 4000$, and spatial resolution was about 80 μm. In Fig. 1and 2a are shown an example of the spectroscopic data in the region of the He_α resonance line. The He_α and its satellites can be seen in the range from 3.85 to 4.15 Å, and are obtained from the fourth order mica crystal reflection. Please note that the He_β, He_γ, and He_δ appear in the He_α spectrum from the fifth order reflection off the mica crystal. The He_γ will be included in the model spectra, although its intensity relative to the He_α was arbitrary and was not used in the spectral analysis.

In order to generate the theoretical spectra, the system of steady state radiative-collisional rate equations was solved for uniform plasma with different plasma parameters [35]. In order to perform a detailed analysis on the Ar He_α and its Li-like satellites, only multicharged argon ions with a total number of bound electrons m=1,2,3 and 4 were taken into account. Atomic configurations with principal quantum numbers $n < 6$ were considered, including auto-ionizing states, for H-, He-, Li- and Be-like ions (25 H-like levels, 59 He-like levels, 334 Li-like levels and 1188 Be-like l levels.) The rate coefficients for the electron collision processes were calculated using a model electron-energy distribution function, which includes a provision for hot electrons [36,12–14].

The x-ray emmision spectra were calculated in the region encompassing the spectral range 3.85 to 4.15 Å. The spectral profiles were calculated using an instrumental width of .001 Å with arbitrary additional broadening when needed. No attempt was made to use line broadening techniques as a plasma diagnostic. Density measurements are primarily obtained by comparing the relative intensity of the He_α resonance line and its intercombination line, indicated as $He_{\alpha 1}$ in Fig. 2a. The bulk temperature and hot electron fraction can be determined from the relative intensity of the Li-like q,r,a-d satellites and the H_α line compared to the other Li-like satellites. The effect of the hot electrons is to enhance the Li-like q,r,a-d

satellites and the He-like lines. See references [12–14] for more information on the effects of hot electrons on Ar K-shell spectra.

Fits of theoretical spectra are compared with experimental data for the spectral region under consideration. The spectrum in Fig. 1 shows emission from many ionization stages and therefore resembles data from experiments where large temperature gradients are observed as well as the presence of hot electrons. Temperature and density gradients are not unexpected since the clusters are immersed in lower density Ar gas which does not absorb the laser energy as efficiently. As a result, the model spectra in the region of the Ar He_α and its Li- and Be-like satellites were generated using two sets of plasma parameters. The case of optimum laser contrast and pulse length of 45 fs is shown in Fig. 2b, the higher temperature component is characterized by a temperature of about 215 eV, with a supercritical density of 2×10^{22} cm^{-3}, and hot electron fraction 1.7×10^{-4}, while a much smaller contribution to the He_α and Li-like emission is characterized by a temperature of $kT = 100 - 130$ eV, $N_e = 3 \times 10^{19}$ cm^{-3}, and hot electron fraction less than 10^{-7}. In Fig. 2c is shown a theoretical profile caculated *without* the effects of hot electrons to demonstrate that all features of the data cannot be fit with a high ($kT = 600$ eV) temperature and no hot electrons. This is particularly true for the Li-like q,r,a-d satellites indicated in Fig. 2a.

X-ray spectral measurements were obtained while varying prepulse contrast for a fixed pulse length of 45 fs, the results of which can be seen in Fig 3. While the temperatures and hot electron fractions declined as contrast was improved, the observed densities were monotonically increasing with contrast. These observations are consistent with previous experiments on solid targets, where the highest densities are achieved with the greatest contrast. With diminishing contrast (greater prepulse), a preplasma has an opportunity to form, causing the target to expand and reach critical density sooner. As a result, the cluster may experience more resonant heating by the main pulse.

In addition, observed electron densities were sensitive to pulse length. Trials were performed using laser pulse lengths between 45 fs and 1.1 ps, using the maximum contrast. The results are shown in Fig. 4. Since the prepulse contrasts was held constant, tempera-

tures and hot electron fractions also stayed approximately constant. The densities, on the other hand, generally increased with decreasing pulse length, reaching a maximum of about 2×10^{22} cm^{-3} for the shortest pulse length used, 45 fs. Similarly to the previous comparison, the energy is deposited before the clusters can expand when a sufficiently short pulse is used. For such time scales, the system may approximate isochoric heating. Also, maximum K-shell emission occurs when a 700 fs laser pulse is used. This result is consistent with results of both Parra, et al., [29] and Zweiback, et al., [28] who achieved maximum emission and absorption, respectively, at approximately 300 fs for argon clusters under similar conditions. Although this conclusion is not immediately obvious, our backing pressure is at least double that used by either group, who used 500 psi (34.5 bar) and 300 psi (20.7 bar) respectively. The increased backing pressure corresponds to increased cluster size and expansion times.

Finally, we note that our temperature and density results show good agreement with calculations using a hydrodynamic model of laser-cluster interaction conducted by Milchberg et al [16]. Since the intensity used in this work is much lower than that used in the current experiment and a 1-D model is employed, we can expect mainly qualitative agreement. In Milchberg's calculation, the peak electron density is found to increase to near solid density (approximately 1×10^{23} cm^{-3}) early in the 130 fs pulse and drop down to critical density (1.7×10^{21} cm^{-3}) at the peak of the pulse. The peak temperature seems to rise to no more than $kT = 400$ eV and drops to a value around 200 eV when the cluster reaches critical density. Except for a short-lived peak in temperature and density, both values seem to drop off after the pulse has passed. These values of temperature and density are roughly consistent with our analysis of the experimental data. Had the spectral analysis shown in this article been conducted without incorporating the effects of hot electrons, the inferred temperature ($\approx$600 eV) would have been too high. This comparison may also indicate that emission from plasmas characterized by supercritical densities occur on time scales comparable to the laser pulse length, while emission from plasmas at or below critical density may last for times longer than the laser pulse length.

In conclusion, we have demonstrated that plasmas characterized by supercritical elec-

tron densities ($\approx N_e = 2 \times 10^{22}$ cm^{-3}) were measured for the first time from Ar cluster interactions with high-intensity lasers. Such densities were achieved using a high-contrast laser pulse, similarly to solid targets, while also using an ultrashort pulse (<100 fs). The ultrashort pulse allowed the laser energy to be deposited before a critical density layer developed. A detailed spectroscopic analysis of cluster plasmas was conducted as pulse length and contrast were varied, allowing us to diagnose electron temperature and density, as well as hot electron fraction. The temperatures and densities obtained from the analysis were consistent with Milchberg's model, suggesting both that accounting for hot electrons in spectroscopic analysis provides an improved diagnosis of cluster plasmas and that Milchberg's model of laser-cluster interaction describes the behavior of cluster plasmas observed in these experiments. Further study of x-ray pulse durations from Ar cluster-plasmas should be pursued, particularly in the case of He_αradiation. Transitions in highly ionized states shows more promise than K_α emission, which is known to have a duration in excess of a picosecond [1,37].

This work was partly supported by the Fond Européen de Développement Economique Régional and the Conseil Régional d'Aquitaine and the U.S. Department of Energy.

REFERENCES

[1] T. Ditmire, T. Donnelly, A. M. Rubenchik, R. W. Falcone, and M. D. Perry. *Phys. Rev A*, 53(5):3379–3402, 1996.

[2] T. Ditmire, J. Zweiback, V. P. Yanovsky, T. E. Cowan, B. Hays, and K. B Wharton. *Nature*, 398:6727, 1999.

[3] A. McPherson, B. D. Thompson, A. B. Borisov, K. Boyer, and C. K. Rhodes. *Nature*, 370:631–4, 1994.

[4] T. Ditmire, R. A. Smith, J. W. G. Tisch, and M. H. R. Hutchinson. *Phys. Rev. Lett.*, 78(16):3121–4, 1997.

[5] Y. L. Shao, T. Ditmire, J. W. G. Tisch, E. Springate, J. P. Marangos, and M. H. R. Hutchinson. *Phys. Rev. Lett.*, 77(16):3343–6, 1996.

[6] T. Ditmire, J. W. G. Tisch, E. Springate, M. B. Mason, N. Hay, R. A. Smith, J. P. Marangos, and M. H. R. Hutchinson. *Nature*, 386:54–6, 1997.

[7] T. Ditmire, J. W. G. Tisch, E. Springate, M. B. Mason, N. Hay, J. P. Marangos, and M. H. R. Hutchinson. *Phys. Rev. Lett.*, 78(14):2732–35, 1997.

[8] E. M. Snyder, S. A. Buzza, and A. W. Castleman Jr. *Phys. Rev. Lett.*, 77(16):3347–50, 1996.

[9] S. Dobosz, M. Schmidt, M. Perdrix, P. Meynadier, O. Gobert, D. Normand, A. Ya. Faenov, A. I. Magunov, T. A. Pikuz, I. Yu. Skobelev, and N. E. Andreev. *JETP Letters*, 68(6):485–91, 1998. English edition.

[10] S. Dobosz, M. Schmidt, M. Perdrix, P. Meynadier, O. Gobert, D. Normand, K. Ellert, T. Blenski, A. Ya. Faenov, A. I. Magunov, T. A. Pikuz, I. Yu. Skobelev, and N. E. Andreev. *JETP*, 88(6):1122–9, 1999. English edition.

[11] J. Zweiback, R. A. Smith, T. E. Cowan, G. Hays, K. B. Wharton, V. P. Yanovsky, and

T. Ditmire. *Phys. Rev. Lett.*, 84(12):2634, 2000.

[12] J. Abdallah Jr., A. Ya. Faenov, I. Yu. Skobelev, A. I. Magunov, T. A. Pikuz, T. Auguste, P. D'Oliviera, S. Hulin, and P. Monot. *Phys. Rev A*, 63:032706, 2001.

[13] G. C. Junkel-Vives, J. Abdallah Jr., F. Blasco, C. Stenz, F. Salin, A. Ya. Faenov, A. I. Magunov, T. A. Pikuz, I. Yu. Skobelev, T. Auguste, P. D'Oliveira, S. Hulin, P. Monot, and S. Dobosz. High-resolution x-ray spectroscopy investigations of fs laser irradiated ar clusters by varying cluster size and laser flux density. *J. Quant. Spectr. and Radiat. Transfer.* to be published.

[14] G. C. Junkel-Vives, J. Abdallah Jr., F. Blasco, C. Stenz, F. Salin, A. Ya. Faenov, A. I. Magunov, T. A. Pikuz, and I. Yu. Skobelev. *Phys. Rev. A*, 64:021201R, 2001.

[15] J.C. Weisheit. In C.F. Barnett and M.F.A. Harrison, editors, *Applied atomic collision physics*, volume 2, page 441. Academic Press, New York, 1984.

[16] H. M. Milchberg, S. J. McNaught, and E. Parra. Plasma hydrodynamics of the intense laser-cluster interaction. submitted to PRE.

[17] J. A. Cobble, G. A. Kyrala, A. A. Hauer, A. J. Taylor, C. C. Gomez, N. D. Delamater, and G. T. Schappert. Kilovolt x-ray spectroscopy of a subpicosecond-laser-excited source. *Phys. Rev. A*, 39(1):454–7, 1989.

[18] C. Y. Cote, J. C. Kieffer, and O. Peyrusse. *Phys. Rev. E*, 56(1):992, 1997.

[19] J. C. Gauthier, J. P. Geindre, P. Audebert, et al. *Phys. of Plasmas*, 4(5):1811, 1997.

[20] A.Ya. Faenov, J. Abdallah, Jr. Clark, R.E.H., J. Cohen, R.P. Johnson, G.A. Kyrala, A.I. Magunov, T.A. Pikuz, I.Yu. Skobelev, and M.D. Wilke. *Proceedings of the SPIE - The International Society for Optical Engineering*, 3157:10–21, 1997.

[21] A.Ya. Faenov, A.I. Magunov, T.A. Pikuz, I.Yu. Skobelev, S.A. Pikuz, A.M. Urnov, J. Abdallah, R.E.H. Clark, J. Cohen, R.P. Jonson, G.A. Kyrala, M.D. Wilke, A. Mak-

simchuk, D. Umstadter, N. Nantel, R. Doron, E. Behar, P. Mandelbaum, J.J. Schwob, J. Dubau, F.B. Rosmej, and A. Osterheld. *Physica Scripta*, vol.T80B:536–8, 1999.

[22] F.B. Rosmej, U.N. Funk, M. Geissel, D.H.H. Hoffmann, A. Tauschwitz, A.Ya. Faenov, T.A. Pikuz, I.Yu. Skobelev, F. Flora, S. Bollanti, P.Di. Lazzaro, T. Letardi, A. Grilli, L. Palladino, A. Reale, G. Tomassetti, A. Scafati, L. Reale, T. Auguste, P. D'Oliveira, S. Hulin, P. Monot, A. Maksimchuk, S.A. Pikuz, D. Umstadter, M. Nantel, R. Bock, M. Dornik, M. Stetter, S. Stowe, V. Yakushev, M. Kulisch, and N. Shilkin. *J. Quant. Spectrosc. Radiat. Transf.*, 65(1-3):477–99, 2000.

[23] T. Auguste, P. D'Oliveira, S. Hulin, P. Monot, J. Abdallah, A. Ya. Faenov, I. Yu. Skobelev, A. I. Magunov, and T. A. Pikuz. *JETP Letters*, 72(2):38–41, 2000. english edition.

[24] J. C. Kieffer, Z. Jiang, A. Ikhlef, C. Y. Cote, and O. Peyrusse. *J. Opt. Soc. Am. B*, 13(1):132, 1996.

[25] K. Eidmann, A. Saemann, U. Andiel, I. E. Golovkin, R. C. Mancini, E. Andersson, and E. Förster. *J. Quant. Spectr. and Radiat. Transfer*, 65:173, 2000.

[26] P. Gallant, Z. Jiang, C. Y. Chien, P. Forget, F. Dorchies, J. C. Kieffer, H. Pépin, O. Peyrusse, G. Mourou, and A. Krol. *J. Quant. Spectr. and Radiat. Transfer*, 65:243, 2000.

[27] U. Andiel, K. Eidmann, and K. Witte. *Phys. Rev. E*, 63:026407, 2001.

[28] J. Zweiback, T. Ditmire, and M. D. Perry. *Physical Review A*, 59(5):R3166, 1999.

[29] E. Parra, E. Alexeev, J. Fan, K. Y Kim, S. J. McNaught, and H. M. Milchberg. *Phys. Rev E*, 62(5):35931, 2000.

[30] E. B. Treacy. *IEEE J. Quantum Elect.*, QE-5(9):454, 1969.

[31] F. Blasco, C. Stenz, F. Salin, A. Ya. Faenov, A. I. Magunov, T. A. Pikuz, and I. Yu.

Skobelev. *Review of Scientific Instruments*, 72(4):1956, 2001.

[32] A.Ya. Faenov et al. unpublished.

[33] A. C. Boldarev, V. A. Gasilov, F. Blasco, F. Dorchiez, C. Stenz, F. Salin, A. Ya. Faenov, T. A. Pikuz, A. I. Magunov, and I. Yu. Skobelev. Modeling of cluster production in jets as a target from high-intensive ultrashort laser interaction. unpublished.

[34] I. Yu. Skobelev, A. Ya. Faenov, B. A. Bryunetkin, et al. *JETP*, 81:692, 1995.

[35] J. Abdallah Jr., R. E. H. Clark, D. P. Kilcrease, G. Csanak, and C. J. Fontes. *AIP Conference Proceedings*, 361, 1996.

[36] J. Abdallah Jr., A. Ya. Faenov, T. A. Pikuz, M. D. Wilke, G. A. Kyrala, and R. E. H. Clark. *JQSRT*, 62:1–11, 1999.

[37] J. Larsson and A. Sjögren. *Review of Scientific Instruments*, 70(5):2253, 1999.

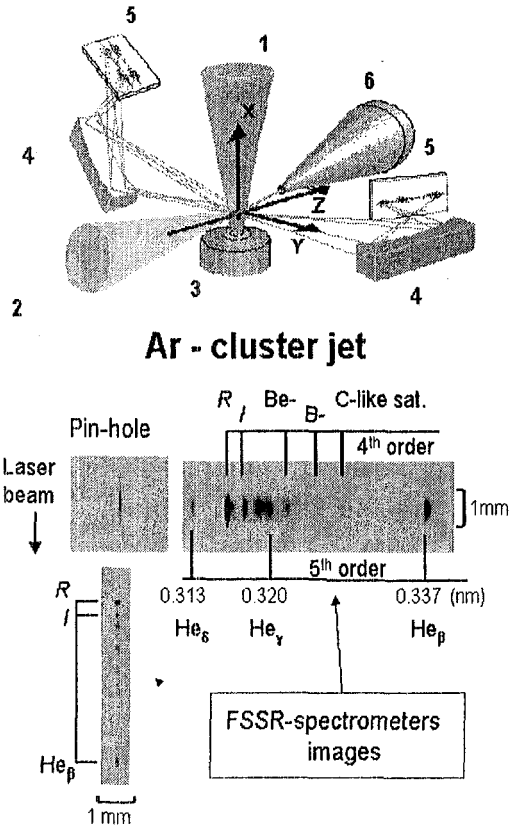

FIG. 1. A schematic of the experimental setup is shown. The various aspects are as follows: (1) the gas jet, (2) the laser beam, (3) focusing spectrographs, (4) RAR-2492 film, (5) CCD camera, (6) pinhole camera. Ar K-shell spectra is shown below. Specific features include: R,I - Resonance and Intercombination lines of He-like Ar. Be-, B- C- satellites of corresponding isoelectronic sequences.

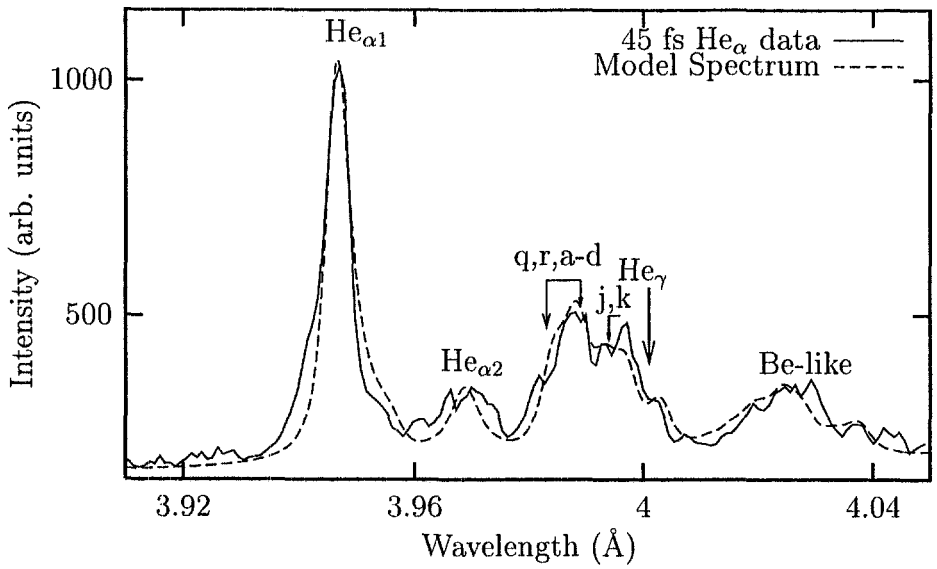
45 fs Heα data
Model Spectrum
Heα1
Heα2
q,r,a-d
j,k
Heγ
Be-like
1000
500
Intensity (arb. units)
3.92
3.96
4
4.04
Wavelength (Å)

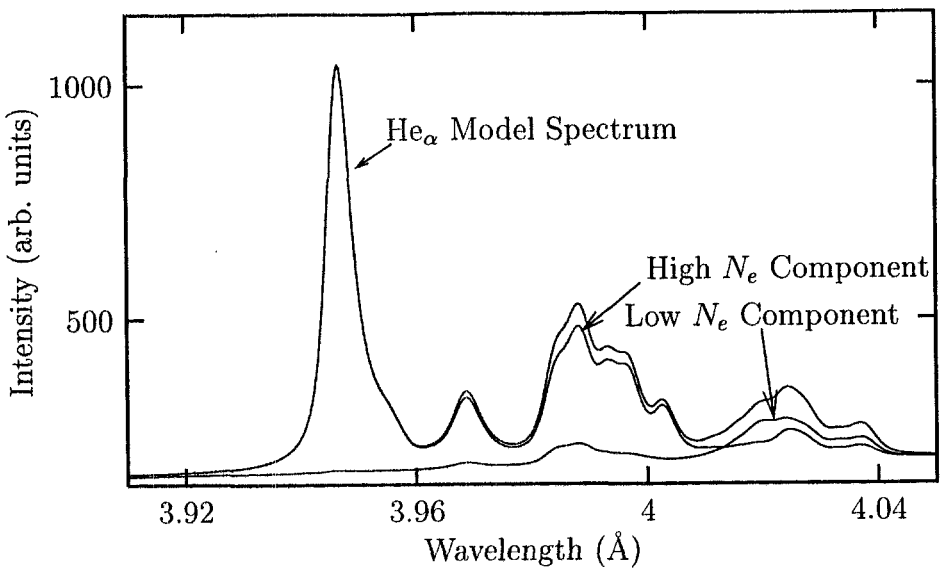
1000
500
Intensity (arb. units)
He$_\alpha$ Model Spectrum
High N_e Component
Low N_e Component
3.92
3.96
4
4.04
Wavelength (Å)

FIG. 2. The Ar K-shell spectrum is shown for the highest contrast and shortest pulse (45 fs). (a) Ar He_α is shown in detail with its Li- and Be-like satellites and the model spectrum. (b) The model spectrum is shown with its two components: the high density contribution ($N_e = 2 \times 10^{22}$ cm^{-3}, $kT = 215$ eV, and $f = 1.7 \times 10^{-4}$) and a low density contribution, ($N_e = 3 \times 10^{19}$ cm^{-3}, $kT = 130$ eV, and $f = 10^{-7}$), where f is the hot electron fraction. (c) The best fit spectrum with a higher temperature ($kT = 600$ eV) with and *without* the effects of hot electrons is shown. Neither is profile a good fit, especially for the q,r,a-d satellites, indicating that the experimental data cannot not be described using a higher temperature.

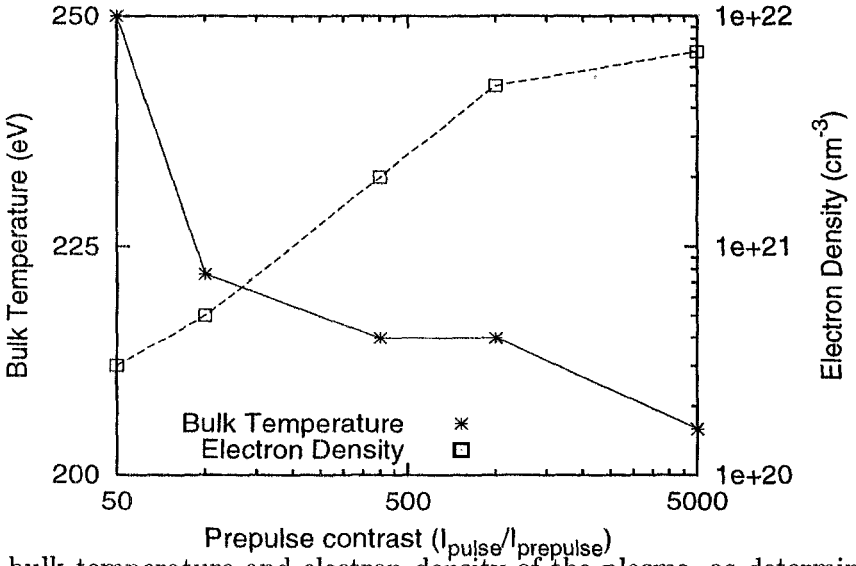

FIG. 3. The bulk temperature and electron density of the plasma, as determined by spectral analysis, as a function of prepulse contrast. The laser pulse length was 45 fs. The density is strongly increasing with contrast, with the temperature decreasing.

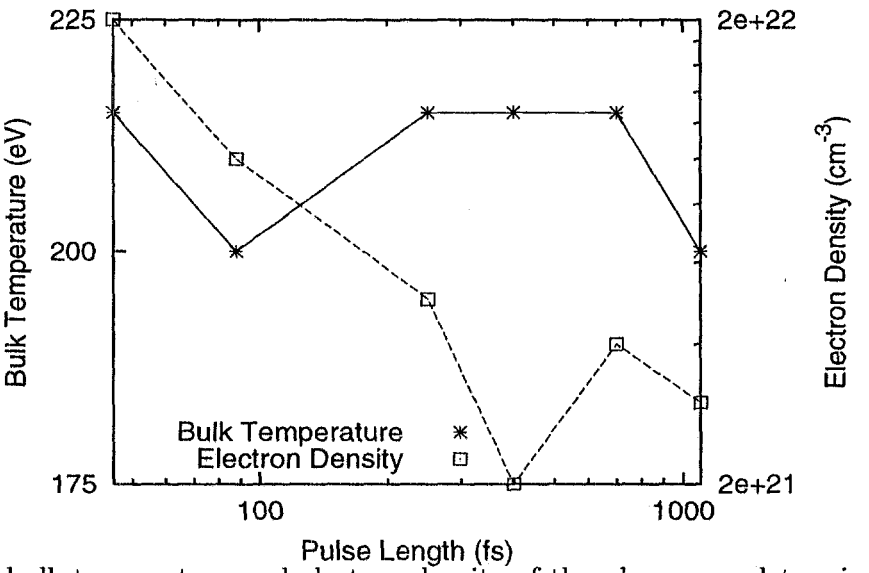

FIG. 4. The bulk temperature and electron density of the plasma, as determined by spectral analysis, as a function of laser pulse length, with maximum contrast. The temperature stays fairly constant, while the density decreases with increasing pulse length.

This research is supported by the Department of Energy under contract W-7405-ENG-36.